Enhanced photoresponse of graphene oxide functionalised SnSe films

Hao Yao, Siwei Luo, Georg S. Duesberg, Xiang Qi, Donglin Lu, Chao Yue, and Jianxin Zhong

---

Articles you may be interested in

Nanostructured SnSe: Synthesis, doping, and thermoelectric properties
Journal of Applied Physics **123**, 115109 (2018); 10.1063/1.5018860

Rhenium-doped MoS_2 films
Applied Physics Letters **111**, 203101 (2017); 10.1063/1.4995220

Making graphene visible
Applied Physics Letters **91**, 063124 (2007); 10.1063/1.2768624

2D-2D tunneling field-effect transistors using WSe_2/$SnSe_2$ heterostructures
Applied Physics Letters **108**, 083111 (2016); 10.1063/1.4942647

Reinvestigation of the thermal properties of single-crystalline SnSe
Applied Physics Letters **110**, 032103 (2017); 10.1063/1.4974348

Record Seebeck coefficient and extremely low thermal conductivity in nanostructured SnSe
Applied Physics Letters **106**, 083902 (2015); 10.1063/1.4913260

Enhanced photoresponse of graphene oxide functionalised SnSe films

Hao Yao,[1,a] Siwei Luo,[1,2,a] Georg S. Duesberg,[2] Xiang Qi,[1] Donglin Lu,[1] Chao Yue,[1] and Jianxin Zhong[1,b]

[1]*Hunan Key Laboratory for Micro-Nano Energy Materials and Devices, Laboratory for Quantum Engineering and Micro-Nano Energy Technology, and School of Physics and Optoelectronics, Xiangtan University, Hunan 411105, People's Republic of China*
[2]*Institute of Physics, EIT 2, Faculty of Electrical Engineering and Information Technology, Universität der Bundeswehr München, Werner-Heisenberg-Weg 39, 85577 Neubiberg, Germany*

The successful synthesis of large-area SnSe films on SiO_2/Si substrate through vapor transport is reported. Based on this we fabricated photodetectors that exhibited a fast response from ultraviolet (UV) to near infrared (NIR) wavelengths. By decorating the SnSe film with graphene oxide quantum dots (GO QDs) the photocurrent and photoresponse time were enhanced significantly over the whole spectrum. Our results indicate that GO functionalised SnSe is a promising material for broadband photodetection. © *2018 Author(s). All article content, except where otherwise noted, is licensed under a Creative Commons Attribution (CC BY) license (http://creativecommons.org/licenses/by/4.0/).* https://doi.org/10.1063/1.5031066

I. INTRODUCTION

In the recent years, two dimensional (2D) materials, containing graphene,[1,2] topological insulators (TIs),[3,4] graphene-like transition-metal dichalcogenides (TMDs),[5,6] hexagonal boron nitride (h-BN),[7] and black phosphorus (BP),[8–10] have drawn extensive attention due to their fascinating electro-optical properties with extensive applications possibilities. Tin selenide (SnSe), appears as a representative of layered IV-VI chalcogenides, which stems from a distorted rock-salt structure with tin and selenium arranged in two adjacent layers to form a 2D planner bilayer (BL) structure. Within the layer, they are combined by weak van der Waals interactions. The binary p-type semiconductor material has application potential, in thermoelectric energy conversion,[11] and lithium-ion batteries.[12] It owns an indirect bandgap and a direct band gap, which are ~0.9 eV and ~1.3 eV, respectively, ideal for photovoltaics and photodetectors with a wide spectral response.[13] Li et al. tested the bandgap and optoelectronic properties of ultrathin SnSe nanosheets and expected it has great potential for photodetectors.[14] Cao et al. successfully synthesized vertical SnSe nanorod arrays to fabricate thermistors and photoresistors, which showed high performance.[15] However, as far as we know, little work has been focused on the application of SnSe for broadband photo-detection so far. Based on this, we fabricated SnSe based photodetectors with exhibited fast response from ultraviolet (UV) up to near infrared (NIR).

However, the indirect bandgap of a material will limit its photo-responsivity and photo-gain. It has been shown that construction of hybrid nanocomposites provides a promising strategy to improve photoresponse performance of the materials with indirect band-gaps. Nazir et al. reported that by the decoration of ZnO QDs, the photoresponse of MoS_2 thin film was improved significantly.[16] Besides, Chen et al. and his colleagues fabricated a photodetector based on graphene/InSe heterostructure and found its photoresponsivity increased by 10^3 times compared to the device without graphene.[17] To enhance the photoresponse of the SnSe, we decorated the sample with GO QDs.

---

[a]These authors contributed equally to this work.

[b]Corresponding author E-mail address: jxzhong@xtu.edu.cn

8, 075123-1

In the past few years, significant progresses have been achieved in SnSe synthesis. For instance, Li et al. used a one-pot synthetic method to produce 1 nm thick and 300 nm large single crystalline SnSe nanosheets.[14] In our preliminary work, we used a facile hydrothermal intercalation and exfoliation route, which can produce thin layer and a large amount thin layers of SnSe, the chemical solution will inevitable induced impurities,[18] S Yuan et al. developed a surfactant-free aqueous solution strategy for the phase-controlled synthesis of SnSe NSs in 2017.[19] However, this strategy still relies on toxic, expensive and air-sensitive Se precursors, as such limit its large-scale application. Recently, we reported the temperature-dependent Raman response of SnSe flakes grown by the vapor deposition method which is simple, direct, pure, and reproducible. Therefore, we used this method to obtain large area SnSe films in current manuscript.

In our work, we report a simple, direct, and low-cost vapor deposition method to obtain large-area SnSe films. Based on this we fabricated SnSe based photodetectors exhibited fast response from ultraviolet (UV) up to near infrared (NIR). To enhance the photoresponse of the SnSe, we decorated the sample with GO QDs and found out the photocurrent and photoresponse time were enhanced significantly over the whole spectrum. The results indicate that SnSe is a promising layer material for photodetection applications, and it is feasible to further enhance its properties by the decoration of GO QDs.

II. EXPERIMENTAL SECTION

A. Synthesis of SnSe film

The SnSe films were synthesized using SiO_2/Si substrate (300 nm SiO_2) in a CVD furnace through vapor phase deposition. To clean the surface of the substrate, we used Piranha solution (H_2SO_4/H_2O_2=7:3) and isopropyl alcohol. As shown in Figure 1(a), SnSe powder (Alfa Aesar, 99.999% purity) was laid in the heating center of the Thermo SCIENTIFIC furnace, and the as-cleaned SiO_2/Si substrate was located downstream at about 9-12 cm away from the heating center. The furnace and then heated to 600 °C in 17 minutes with 95:5 Ar/H_2 gas flow of 100 standard cubic centimeter per minute (sccm) and then maintained for 30 minutes before it naturally cooled down.
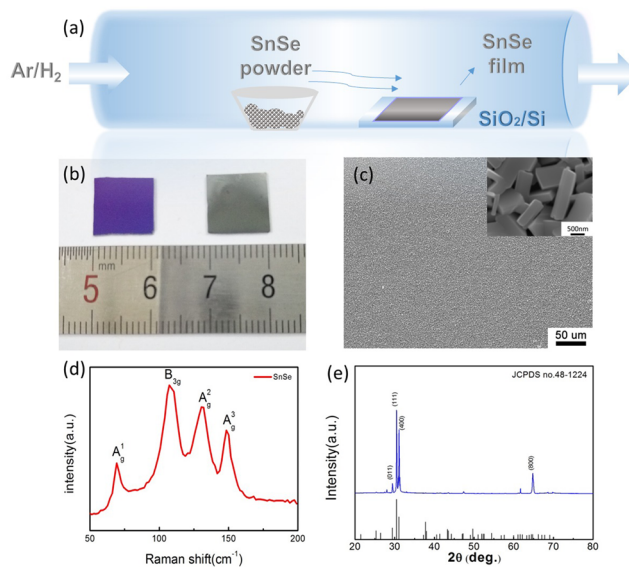

FIG. 1. (a) The schematic of the vapor phase deposition growth system to prepare SnSe film. (b) Photograph of the bare SiO_2/Si substrate and the as-grown SnSe film. (c) The typical SEM images of the SnSe film. (d) Raman spectra of the SnSe film. (e) XRD pattern of the SnSe film.

B. Characterization

XRD (Cu K α radiation) was employed to measure the crystal structure of the SnSe films. For the morphologies and microstructures, we used scanning electron microscope (SEM, Tescan Vega3 SBH) to characterize of the as-prepared SnSe thin films. Raman spectra were obtained at room temperature with excitation laser wavelength of 532 nm with 100x objective lens by Renishaw Invia Raman microscope. UV absorption spectrum was measured by UV-visible spectrophotometer (UV-2550) in the resolution of 0.1 nm.

C. Device fabrication

We fabricated a two-electrode device, in which the contact electrodes were deposited with Ag on the SnSe film. Then the GOQDs solution (XF NANO, 20 mg/ml) was dropped onto the SnSe devices with a spin coater followed by a heat treatment at 80°C for 5 min.

D. Electric and photoelectric measurements

Electric and Photoresponse measurements were measured by using a Keithley 2400 source. The photocurrents of the photodetectors were measured at 0.01 V. The wavelengths of the excitation laser were 405 nm, 532 nm, 650 nm, 808 nm and 850 nm, excited at room temperature.

III. RESULTS AND DISCUSSION

A digital photograph of the bare SiO$_2$/Si substrate (left) and a SiO$_2$/Si substrate deposited by SnSe film (right) is depicted in Figure 1(b). The SnSe film is silver grey, which is completely distinguishable from the bare substrate. Figure 1(c) exhibits the typical SEM images of our as-synthesized SnSe film, which is formed by closely stacked SnSe sheets.

Generally, Raman spectra were used to study the quality and constitute of the as-prepared SnSe film. SnSe possesses two major characteristic planar vibration modes, B$_{3g}$ and A$_g$. As we can see in Fig. 1(d), four intense peaks are clearly observed at 69.6, 107.6, 130.9 and 149.0 cm^{-1}, which are corresponding to A_g^1, B_{3g}, A_g^2, and A_g^3 modes, respectively. These four peaks are in agreement with the previous reports.[20] The laser power was set at a very low level in case it would cause any damages to our sample. Powder XRD pattern was carried out to illustrate the phase structure of our SnSe film. As shown in Figure 1(e), the whole diffraction peaks are identified with JCPDS no. 48-1224, Pnma, which is the orthorhombic SnSe standard spectrum containing the unit cell of a =11.498 Å, b = 4.153 Å, and c =4.440 Å.

I-V characteristics of the SnSe film photodetector irradiated by a monochromatic light of varied light intensity were measured and are shown in Figure 2(a). From Figure 2(a) we can find that under 650 nm illumination, the photocurrent of our device was enhanced obviously, especially under high voltage bias. Besides, our results demonstrate an asymmetrical and nonlinear I-V behavior, indicating that a Schottky contact has emerged. Moreover, under the same voltages, the photocurrent got enhanced with the increase of the energy power of the laser. For the sake of gain insight to the photo-response property of the SnSe film, time-dependent photocurrent characteristics were investigated under various laser wavelengths, which covered from the UV to near-infrared, including 405 nm, 532 nm, 650 nm, 808 nm and 850 nm, respectively. The measurements were performed under various illuminations with the applied potential of 0.01 V as presented in Figure 2(b) (light power: 50 mW). One can find from Figure 2(b) that the device showed a good broadband response from 405 nm to 850 nm and exhibited a rapid response time and good reproducibility, which demonstrates that SnSe can be employed as an up-and-coming material for broadband photo-detection from UV to near-infrared (NIR). In addition, the SnSe film displayed a strong and wide absorption spectrum from 200 to 900 nm as shown in figure 2(c). Noteworthy, with the increase of the wavelength, the photocurrent was enhanced continuously and reached the maximum value at 650 nm, and then decreased from 808 nm and continuously declined up to 850 nm wavelength, which is consistent with the absorption spectrum in figure 2(c). Generally, lights with larger energy, that is, in shorter wavelength, are able to excite more electrons from the valence band to the conduction band, which will contribute more to the photocurrent. However, there is a tradeoff between the photon energy and the amount of the
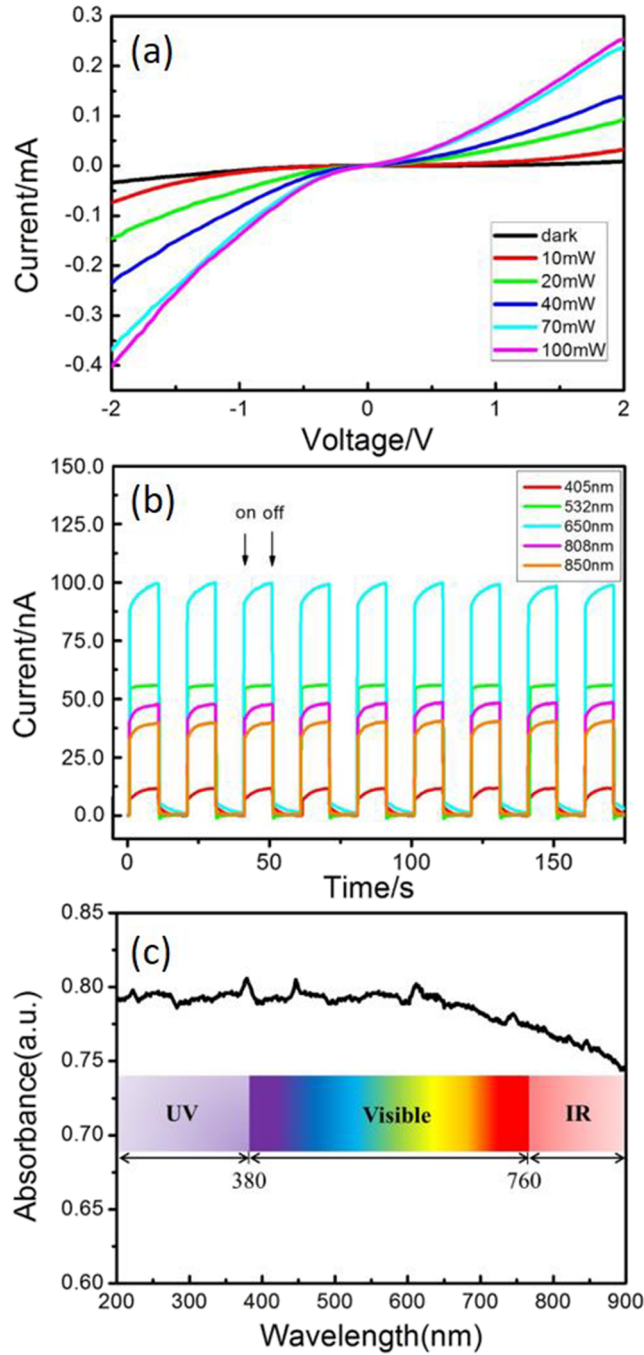
FIG. 2. (a) I-V characteristics of the SnSe film photodetector. (b) The time-dependent photocurrent measurements of the SnSe photodetector. (c) The absorption spectrum of SnSe film.

photo-generated carriers. Under a constant incident power, the increase of the photon energy is at the expense of the number of the carriers, which will finally compromise the photocurrent's increase. In this case, the photocurrent of our samples reached a maximum value at 650 nm, where the tradeoff was optimized.[21,22] Therefore, our results show that the photodetector based on SnSe is competitive to those based on MoS_2, WS_2, GaSe, GaTe, and GaS, which only response under visible or ultraviolet light because of their larger bandgaps.[23–26]
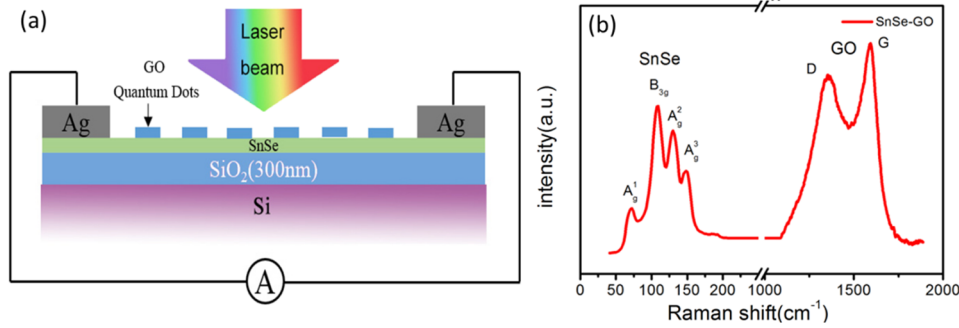
FIG. 3. (a) The cross-sectional view of the photodetector based on GO-QDs/SnSe film. (b) Typical Raman spectrum of the GO-QDs/SnSe film.

To enhance the photoresponse intensity, we fabricated a GOQDs decorated SnSe film photodetectors, as schematically illustrated in Figure 3(a). As shown in Figure 3(b), the co-existence of the Raman peaks of SnSe and GO QDs confirmed the successful decoration GO QDs on SnSe films. We now compare the photoresponse properties of photodetectors based on pure SnSe films and GO/SnSe hybrid film without sweeping voltage. When GO QDs were distributed on the SnSe film, the p-type SnSe film and n-type GO quantum dots will form into separated p-n junctions. We used a laser of 650 nm wavelength to investigate the enhancement of the light response in the GO-QDs/SnSe photodetector with GO-QDs solution (5 ml). As depicted in Figure 4(a), photocurrent increased significantly with the decoration of the GO QDs, the photocurrent was two times larger compared to the pure SnSe film when 5 mL GO QDs solution was used. We also found that adsorption of GO QDs did not substantially affect the speed and stability of the photoresponse. It is worth noting that all the time-dependent photocurrent measurements were also tested with the same light power at room temperature. Thus, decoration of GO QDs onto SnSe film can be used to effectively enhance the photoresponse of pure SnSe films.

To better understand the mechanism of the enhancement in the photodetector of GO-QDs/SnSe hybrids, we present a diagram with energy band of the hybrid in Figure 4(b). As both SnSe and GO QDs are semiconductors with narrow bandgaps, it is of great importance that when they contact and interact with each other, we need to build a relative energy levels in order to indentify the band bending and carrier transfer direction.[27] After GO QDs are dropped on a SnSe film, it results in formation of built-in field at the p-n junction. Under illumination of visible light, the photo-excited electrons and holes will immediately separate at the interface of SnSe and GO QDs, leading to current increase.

Figure 5(a) - (d) gives the time-dependent photoresponse measurement of the photodetectors based on pure SnSe and GO-QDs/SnSe (1 ml GO QDs solution distributed on the SnSe film) by
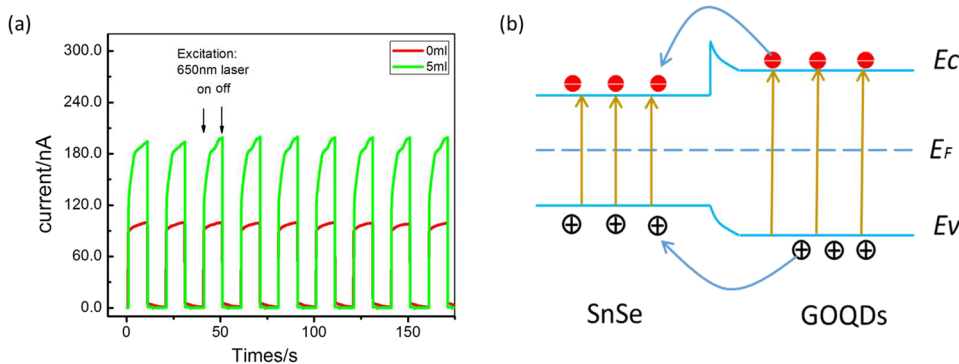

FIG. 4. (a) Photoresponse of the SnSe film with decoration of GO QDs. (b) Energy band diagram of the interface between SnSe and GO QDs.
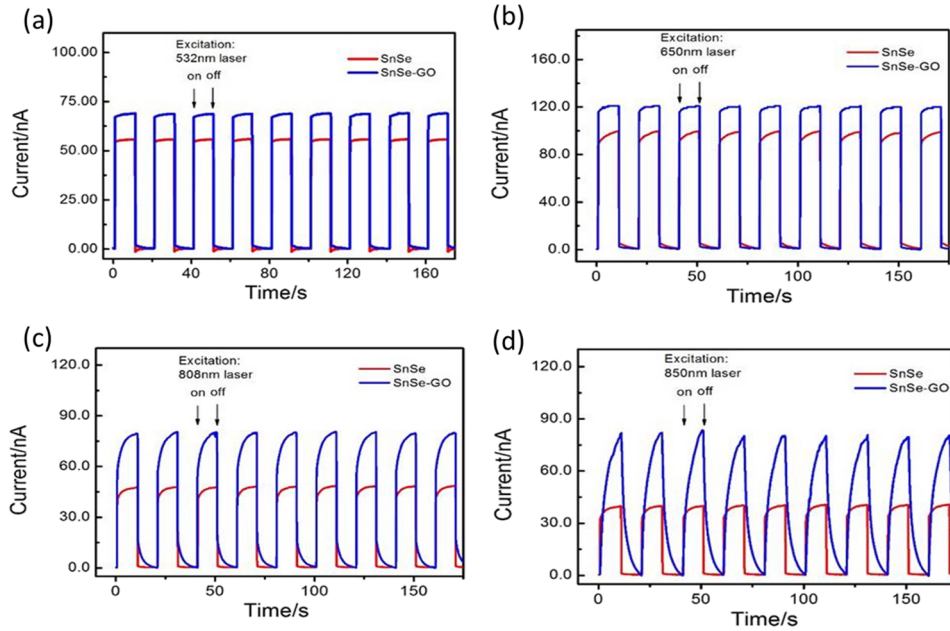
FIG. 5. (a)-(d) The measured time-dependent photoresponse of pure SnSe film and GO-QDs/SnSe film under 532 nm, 650 nm, 808 nm, and 850 nm, respectively.

periodically switching on and off laser light with wavelengths of 532 nm, 650 nm, 808 nm, and 850 nm, severally. In comparison to the device with pure SnSe, the device based on GO-QDs/SnSe hybrid exhibited obvious enhancement of photoresponse in all laser wavelengths we used. With the increase of wavelength, the enhancement of photoresponse by decoration of GO QDs became more obvious. Under the excitation of 850 nm, the photocurrent was nearly 3 times larger than that of the device based on pure SnSe. Compared with 532 nm, 650 nm, and 808 nm wavelengths, the photocurrent under 850 nm laser irradiation show higher enhancement. This might explained by the higher optical absorption in the 800-1300 nm region.[28–30]

Response time is a pivotal parameter to judge the performance of a photodetector. Thus, the photoresponse times of the pure SnSe and GO-QDs/SnSe devices were investigated for comparison and the results are shown in Figures 6(a) and (b). The experimental data (squares) are fitted (solid lines) to the following equation:[31]

$$I(t) = I_0 + A[\exp(-t/\tau)],$$

where A is a scaling constant, τ is the photoresponse time when light source switches on or off, and I_0 represents the original current. From the fitting data in Figures 6(a) and (b) under irradiation of
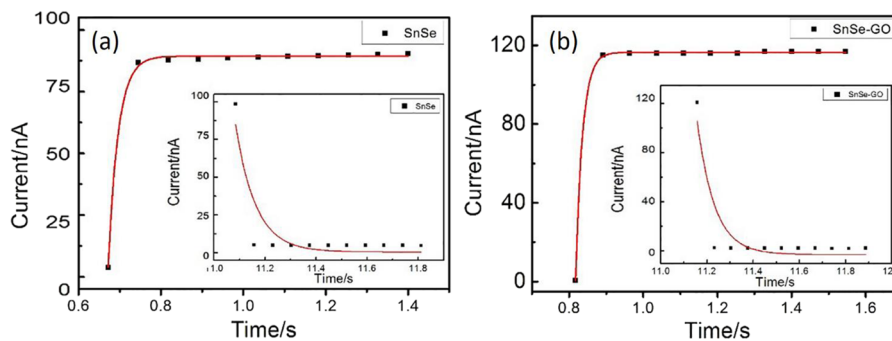

FIG. 6. Time-resolved photocurrent of (a) the SnSe photodetector and (b) the GO-QDs/SnSe photodetector under irradiation of 650 nm laser.

TABLE I. Comparison of SnSe-based photodetector reported in the literature.

Material	Synthesis method	Light	Response time (s)	Ref.
SnSe films	Hydrothermal	visible	0.19	1
SnSe Nps-Graphene	Solvothermal	White light	1	2
SnSe nanorods	Solvothermal	White light	3	3
SnSe film	Vapor deposition	650 nm	0.24 (rise) 0.79 (decay)	present
SnSe film-GO QDs	Vapor deposition	650 nm	0.18(rise) 0.75 (decay)	present

650 nm laser, the response time constants of pure SnSe for rise and decay are 24 ms and 79 ms respectively, which are reduced to 18 ms and 75 ms respectively after incorporation of GO QDs. These results are superior compared to other published SnSe based photodetector samples, which have presented in Table I.[14,32,33] The obvious shortening of response times is determined by the efficient charge transfer between the SnSe film and the GO QDs. Therefore, decorating GO QDs on SnSe provides a simple and valid method to improve the photoresponse property of the photodetector based on SnSe film, which can not only enhance the photocurrent remarkably but also significantly decrease the response time.

IV. CONCLUSION

In this work, we synthesized SnSe films on SiO_2/Si controllably by a simple vapor deposition method which without any catalyst. The resulting large-scale SnSe films allowed easy fabrication of photodetector devices. We investigated the photoresponse of these at different wavelengths from UV to NIR, and found that it was fast, stable, and reversible, indicating that SnSe is a promising material for broadband applications. Moreover, we found that decorating GO QDs on SnSe can not only enhance the photocurrent remarkably but also significantly decrease the response time, offering a facile and effective method to improve the characteristics of the photodetectors based on SnSe films.

ACKNOWLEDGMENTS

[1] K. S. Novoselov, A. K. Geim, S. V. Morozov, D. Jiang, Y. Zhang, S. V. Dubonos, I. V. Grigorieva, and A. A. Firsov, Science **306**, 666 (2004).
[2] C. Rao, H. R. Matte, and K. Subrahmanyam, Accounts of Chemical Research **46**, 149 (2012).
[3] A. Zhuang, J. J. Li, Y. C. Wang, X. Wen, Y. Lin, B. Xiang, X. Wang, and J. Zeng, Angewandte Chemie **126**, 6543 (2014).
[4] P. Sengupta, T. Kubis, Y. Tan, M. Povolotskyi, and G. Klimeck, Journal of Applied Physics **114**, 043702 (2013).
[5] K. F. Mak, C. Lee, J. Hone, J. Shan, and T. F. Heinz, Physical Review Letters **105**, 136805 (2010).
[6] H. Zeng, J. Dai, W. Yao, D. Xiao, and X. Cui, Nature Nanotechnology **7**, 490 (2012).
[7] A. Nag, K. Raidongia, K. P. Hembram, R. Datta, U. V. Waghmare, and C. Rao, ACS Nano **4**, 1539 (2010).
[8] G.-C. Guo, D. Wang, X.-L. Wei, Q. Zhang, H. Liu, W.-M. Lau, and L.-M. Liu, The Journal of Physical Chemistry Letters **6**, 5002 (2015).
[9] M. Engel, M. Steiner, and P. Avouris, Nano Letters **14**, 6414 (2014).
[10] H. Yuan, X. Liu, F. Afshinmanesh, W. Li, G. Xu, J. Sun, B. Lian, A. G. Curto, G. Ye, and Y. Hikita, Nature Nanotechnology **10**, 707 (2015).
[11] L.-D. Zhao, S.-H. Lo, Y. Zhang, H. Sun, G. Tan, C. Uher, C. Wolverton, V. P. Dravid, and M. G. Kanatzidis, Nature **508**, 373 (2014).
[12] M.-Z. Xue, J. Yao, S.-C. Cheng, and Z.-W. Fu, Journal of the Electrochemical Society **153**, A270 (2006).
[13] M. A. Franzman, C. W. Schlenker, M. E. Thompson, and R. L. Brutchey, Journal of the American Chemical Society **132**, 4060 (2010).

[14] L. Li, Z. Chen, Y. Hu, X. Wang, T. Zhang, W. Chen, and Q. Wang, Journal of the American Chemical Society **135**, 1213 (2013).

[15] J. Cao, Z. Wang, X. Zhan, Q. Wang, M. Safdar, Y. Wang, and J. He, Nanotechnology **25**, 105705 (2014).

[16] G. Nazir, M. F. Khan, I. Akhtar, K. Akbar, P. Gautam, H. Noh, Y. Seo, S.-H. Chun, and J. Eom, RSC Advances **7**, 16890 (2017).

[17] Z. Chen, J. Biscaras, and A. Shukla, Nanoscale **7**, 5981 (2015).

[18] H. Qiao, Z. Huang, X. Ren, H. Yao, S. Luo, and P. Tang, Journal of Materials Science **53**(6), 4371–4377 (2018).

[19] S. Yuan, Y. H. Zhu, W. Li, S. Wang, D. Xu, L. Li *et al.*, Advanced Materials **29**(4), 1602469 (2018).

[20] S. Zhao, H. Wang, Y. Zhou, L. Liao, Y. Jiang, X. Yang, G. Chen, M. Lin, Y. Wang, and H. Peng, Nano Research **8**, 288 (2015).

[21] J. M. S. G. W. Y. J. D. Yao, Scientific Reports **5**, 12320 (2015).

[22] X. Hu, X. Zhang, L. Liang, J. Bao, S. Li, W. Yang, and Y. Xie, Advanced Functional Materials **24**, 7373 (2015).

[23] O. Lopez-Sanchez, D. Lembke, M. Kayci, A. Radenovic, and A. Kis, Nature Nanotechnology **8**, 497 (2013).

[24] N. Perea-López, A. L. Elías, A. Berkdemir, A. Castro-Beltran, H. R. Gutiérrez, S. Feng, R. Lv, T. Hayashi, F. López-Urías, and S. Ghosh, Advanced Functional Materials **23**, 5511 (2013).

[25] P. Hu, Z. Wen, L. Wang, P. Tan, and K. Xiao, ACS Nano **6**, 5988 (2012).

[26] S. Yang, Y. Li, X. Wang, N. Huo, J.-B. Xia, S.-S. Li, and J. Li, Nanoscale **6**, 2582 (2014).

[27] Z. Jia, J. Xiang, F. Wen, R. Yang, C. Hao, and Z. Liu, ACS Applied Materials & Interfaces **8**, 4781 (2016).

[28] J. Kim, F. Kim, and J. Huang, Materials Today **13**, 28–38 (2010).

[29] L. Huang *et al.*, Carbon **49**, 2431–2436 (2011).

[30] J. T. Robinson *et al.*, Journal of the American Chemical Society **133**, 6825–6831 (2011).

[31] B. Chitara, S. Krupanidhi, and C. Rao, Applied Physics Letters **99**, 113114 (2011).

[32] J. Liu *et al.*, Nanoscale Research Letters **12**, 259 (2017).

[33] A. S. Pawbake, S. R. Jadkar, and D. J. Late, Materials Research Express **3**, 105038 (2016).